Published in final edited form as:
J Mater Chem B Mater Biol Med. 2013 December 14; 1(46): 6359–6364. doi:10.1039/C3TB21104E.

Metal Chelating Crosslinkers Form Nanogels with High Chelation Stability

Jacques Lux[#a], **Minnie Chan**[#a], **Luce Vander Elst**[b], **Eric Schopf**[a,c], **Enas Mahmoud**[a], **Sophie Laurent**[b], and **Adah Almutairi**[a,*]

[a] Skaggs School of Pharmacy and Pharmaceutical Sciences. KACST-UCSD Center of Excellence in Nanomedicine. Laboratory of Bioresponsive Materials, University of California, San Diego. 9500 Gilman Dr., 0600, PSB 2270, La Jolla, CA-92093-0600, United States.

[b] Department of General, Organic and Biomedical Chemistry, NMR and Molecular Imaging Laboratory, University of Mons, 7000 Mons, Belgium.Address, Address, Town, Country.

[#] These authors contributed equally to this work.

Abstract

We present a series of hydrogel nanoparticles (nanogels) incorporating either acyclic or cyclic metal chelates as crosslinkers. These crosslinkers are used to formulate polyacrylamide-based nanogels (diameter 50 to 85 nm) yielding contrast agents with enhanced relaxivities (up to 6-fold greater than Dotarem®), because this nanogel structure slows the chelator's tumbling frequency and allows fast water exchange. Importantly, these nanogels also stabilize Gd^{3+} within the chelator thermodynamically and kinetically against metal displacement through transmetallation, which should reduce toxicity associated with release of free Gd^{3+}. This chelation stability suggests that the chelate crosslinker strategy may prove useful for other applications of metal-chelating nanoparticles in medicine, including other imaging modalities and radiotherapy.

Introduction

Nanogels, nanoscale hydrogel particles formed by chemically or physically crosslinked polymer chains, have attracted much attention in recent years for their high drug-carrying capacity, environmental responsiveness, and stability in aqueous media. [1-2] While they have been employed in several studies to deliver small therapeutic agents [3-4] and biomacromolecules, [5-6] their advantages for use as biomedical imaging agents, such as water access throughout the particle [7] and protection of the payload have not been thoroughly explored.

Metals have many applications in medicine, including as contrast agents in multiple biomedical imaging modalities (PET, MRI), and as radiotherapeutics. Incorporating metals into nanogels can impart properties useful in medicine. However, no versatile and reproducible chemistry yet exists to incorporate metals into nanogels in a stable manner that is of clinical relevance. Clinical development of high-contrast magnetic resonance imaging (MRI) agents is an important area of investigation that relies on Gd^{3+} chelates. Gd based MRI agents could allow tissue- or disease-specific imaging using this accurate diagnostic

[*] Tel: (858) 246 0871; aalmutairi@ucsd.edu.
[c]Current Address: Librede Inc, 570 Westwood Plaza, Los Angeles, CA 90095

[†]Electronic Supplementary Information (ESI) available: Synthesis procedures. Nanogels preparation. MTT assay. MRI Phantoms. Transmetallation, relaxivity and Dynamic Light Scattering (DLS) measurements. See DOI: 10.1039/b000000x/

imaging modality capable of providing submillimeter spatial resolution and unrivalled soft tissue contrast. [8-10] Previously employed strategies combining Gd^{3+} chelates with nanogels include the encapsulation of small contrast agent molecules inside an electrostatically crosslinked polymer [11] or the post polymerization functionalization of nanogels with contrast agents, [12] both of which enhance relaxivity by slowing the chelates' molecular tumbling rate. [14, 15] These designs follow the example of numerous other groups that attach Gd^{3+} chelates to high molecular weight macromolecules, including dendrimers, [13-16] polymers, [17-19] micelles [20-21] and *metallostars* [22] or bind them to micro- [23] or nanoparticles [24-25] or proteins through covalent [26-30] or non-covalent interactions. [31-33]By using gadolinium complexes directly as crosslinkers, the whole nanoparticle incorporates contrast agents, in contrast to post-functionalized nanoparticles or gadolinium-based inorganic nanoparticles, in which only surface gadolinium can relax water protons. This strategy also allows us to keep the nanogel surface available for further functionalization, for example with targeting agents. We also hypothesized that incorporating the contrast agent into a macromolecular network as a crosslinker would further increase rigidity and thus relaxivity. Importantly, metal chelating crosslinkers can be used with a variety of metals, such as radioisotopes for positron emission tomography or cancer radiotherapy. [34]

The design of the target crosslinker **1** (Figure 1) was based on a diethylenetriaminepentacetatic acid (DTPA) and was first selected because of its ease of synthesis. The second crosslinker structures were selected for their potential for greater safety *in vivo*; it has been reported that cyclic structures are more stable than DTPA, [35] better protecting and binding the central Gd^{3+}. A cyclic crosslinker would thus decrease toxicity, which can increase the risk of nephrogenic systemic fibrosis (NSF) via transmetallation with endogenous ions such as zinc or copper and resulting release of free Gd^{3+}. Thus we decided to design two other crosslinkers based on the 1,4,7,10-tetraazacyclododecane-1,4,7,10-tetraacetic acid (DOTA) chelating agent. The design of these macrocyclic crosslinkers **2** and **3** (Figure 1) was based on a DOTA unit bearing a bisacrylamide moiety. The DOTA macrocycle is *C*-substituted in order to avoid any interference with the coordination site of the ligand. This choice is based on previous observations that chelates with a hydration number greater than one are relatively unstable; $q = 1$ for all commercial agents. Therefore, though other designs allow a greater hydration number, which yields higher relaxivity, [36-39] we chose *C* substitution to minimize dechelation. Furthermore, incorporating the chelate into a nanogel both enhances relaxivity by limiting movement and improves Gd^{3+} chelating stability by reducing access of other metal ions. To the best of our knowledge, this work is the first example of nanogels incorporating DOTA chelating agents as crosslinkers.

Herein we report the development of model polyacrylamide (PAA)-based nanogels incorporating DTPA- and DOTA-based crosslinkers. Given the size of these nanogels (<100 nm), which should allow prolonged circulation, these chelators should be useful in the development of biodegradable nanoparticles for a number of biomedical applications involving metals.

Results and discussion

Synthesis of the crosslinkers

Crosslinker **1** was obtained in a one-step synthesis by reacting commercially available DTPA-bisanhydride with N-(3-aminopropyl) methacrylamide hydrochloride in the presence of triethylamine. The adopted strategy for the synthesis of the two DOTA-based crosslinkers **2** and **3** was convergent (Scheme 1). The *C*-substituted protected DOTA derivatives **5** and **7** were prepared in 4 and 5 steps, respectively, according to a procedure reported in the literature. [40] In parallel, the bisacrylamide derivatives **4** and **9** were synthesized in one or

two steps from the commercial 3,5-diaminobenzoic acid and 3,5-dinitroiodobenzene, respectively. The latter was first reduced with tin chloride to give the 3,5-diaminoiodobenzene **8**. The two diamino compounds were acrylated by using acryloyl chloride under Schotten-Baumann conditions (two-phase solvent system) to give **4** and **9**. These bisacrylamide derivatives were then coupled with the protected DOTA derivatives **5** and **7** via coupling reactions: an ester coupling reaction to form the protected crosslinker **6**, and a Sonogashira cross-coupling reaction to form the protected crosslinker **10**. Finally, the two target crosslinkers **2** and **3** were obtained after a TFA deprotection of the tert-butyl ester functions of **6** and **10**.

Nanogel Preparation

The crosslinkers **1**, **2** and **3** were chelated using $GdCl_3$ and heating at 40 °C at pH 6. Excess gadolinium was removed by adding the chelating resin Chelex-100 and filtering the solution. The gadolinium complexes **1**Gd(III), **2**Gd(III) and **3**Gd(III) were then used to prepare polyacrylamide-based nanogels PAA/**1**Gd(III), PAA/**2**Gd(III) and PAA/**3**Gd(III) through an inverse emulsion process using ammonium persulfate (APS) as the initiator and by adding tetramethylethylenediamine (TMEDA) to control the radical polymerization rate (Figure 2).

Nanogel characterization

The nanogels obtained were characterized by dynamic light scattering (DLS) in order to evaluate their hydrodynamic volume and size distribution (Figure 3). PAA/**1**Gd(III) had an average size of 65 nm with a polydispersity index (PDI) of 0.16, PAA/**2**Gd(III) and PAA/**3**Gd(III) were on average 54 nm and 85 nm in diameter with PDI values of 0.25 and 0.39, respectively.

Nanogels were then visualized (Figure 4) by transmission electron microscopy (TEM). Spherical nanogel particles with smaller sizes were observed, which is in accordance with the hydrodynamic sizes measured by DLS. Spherical voids seen on the TEM microphotographs are most likely generated by water escaping from the nanogel upon placement under vacuum and irradiation by the electron beam..

To evaluate the effect of nanogels on cell viability, murine macrophages were incubated with PAA/**1**Gd(III), PAA/**2**Gd(III) and PAA/**3**Gd(III) at various concentrations, and cytotoxicity was measured by MTT assay (Figure S1). From the MTT assay results, it appears that PAA/**1**Gd(III), PAA/**2**Gd(III) and PAA/**3**Gd(III) are well tolerated by the cells at concentrations up to 100 μg/ml.

Relaxivity studies

In order to test our central hypothesis, the relaxivity values of all Gd^{3+} complexes (crosslinkers alone and nanogels incorporating crosslinkers **1**, **2,** and **3**) were calculated. T_1 was measured at 60 MHz (1.41 T), 37 °C in PBS buffer and exact concentrations of Gd^{3+} were measured by inductively coupled plasma atomic emission spectroscopy (ICP-AES). Under these conditions, the clinically used contrast agents Magnevist® (DTPA-Gd^{3+} complex) and Dotarem® (DOTA-Gd^{3+} complex) had relaxivities of 3.6 ± 0.3 mM^{-1s-1} and 2.9 ± 0.3 mM^{-1s-1}, respectively. Proton NMRD profiles were also recorded at 37 °C and analyzed using the classical inner sphere and outer sphere theories (Figure 5). As expected from its larger molecular weight, the complexed crosslinker **1**Gd(III) has a larger relaxivity than Magnevist®. The larger value of the fitted water residence time agrees with previous results showing that replacement of carboxylic groups with amides reduces the water exchange rate. [1, 41] The incorporation of the complexed crosslinker **1**Gd(III) into nanogels resulted in an increase of relaxivity from 4.8 ± 0.2 $mM^{-1}s^{-1}$ for the crosslinker alone to 9.7 ± 0.5 $mM^{-1}s^{-1}$ for the corresponding PAA nanogel at 60 MHz and 37°C. This corresponds

to a 2-fold improvement in relaxivity over Magnevist® after incorporation of the DTPA as a crosslinker. The decrease in mobility of the Gd complex in the nanogels was further confirmed by the NMRD profiles showing a "hump" between 10 and 100 MHz. The r_1 increase is lower than expected for PAA/**1**Gd(III) due to the slow water exchange rate resulting from the presence of the amide chelating groups.

As expected, since the substitution of the DOTA macrocycle would slow molecular tumbling, our complexed crosslinkers **2**Gd(III) and **3**Gd(III) exhibited higher relaxivities than Dotarem®, of 4.3 ± 0.2 $mM^{-1}s^{-1}$ and 5.0 ± 0.3 $mM^{-1}s^{-1}$, respectively, at 60 MHz. The slightly higher relaxivity of **3**Gd(III) compared to **2**Gd(III) could be explained by its higher rotational correlation time τ_R (Table S1) corresponding to a slightly slower tumbling frequency. As anticipated, the NMRD profile shows that the τ_M, τ_{SO} and τ_V values are quite similar for both complexes and comparable to those of Gd-DOTA (Table S1). The relaxivity of nanogels incorporating **2**Gd(III) and **3**Gd(III) was greater than that of the complexed crosslinkers alone, at 17.6 ± 0.9 $mM^{-1}s^{-1}$ and 14.8 ± 0.7 $mM^{-1}s^{-1}$, respectively. This 3 to 4-fold increase in relaxivity can be explained by the relative rigidity of the system after crosslinking. These r_1 values are 5.1 to 6.1-fold improvements over Dotarem®. While these enhancements are limited by the slower water exchange rate in the nanogels, the faster water exchange rate as compared to PAA/**1**Gd(III) results in a faster relaxation rate of these two DOTA-based nanogels.

Based on the density of our nanogels (1.016 g/mL; see ESI), the Gd concentration, and the average nanoparticle volume (calculated from the nanoparticle size measured by DLS), we calculated the number of Gd^{3+} per particle to be 134. This value allowed us to obtain the relaxivity per particle, which was 2352 $mM^{-1}.s^{-1}$ in the case of PAA/**2**Gd(III).

Although the tumbling frequency of the crosslinker in the nanogel is reduced because the attachment of the bismethacrylamide or bisacrylamide linkers restricts each chelate's rotation, the motions of the linkers are still rapid. This internal flexibility becomes the limiting factor for further reduction in tumbling frequency and increase in relaxivity.[42] This also explains the similar r_1 among nanogels with different crosslinking densities (see Figure S2). These nanogels have an overall denser structure at a higher crosslinking density; however, locally, the flexibility of the linkers remains high. As a result, increasing crosslinking density has no significant effect on r_1.

To be clinically translatable, an MRI contrast agent should minimize release of toxic Gd, which occurs mainly through transmetallation of Gd with endogenous metal ions. [7, 43-44] This released Gd^{3+} can accumulate in the body, sometimes causing nephrogenic systemic fibrosis, especially in patients with reduced kidney function. [43-44] Among the endogenous ions, Zn^{2+} is most likely to displace Gd^{3+} because of its relatively high concentration *in vivo*, high affinity to metal chelates, and similar radius to that of Gd^{3+}. The stability of all the chelated crosslinkers and their corresponding nanogels toward transmetallation was evaluated by monitoring their paramagnetic longitudinal relaxation rate $1/T_1$ over time in the presence of other metal ions (Figure 6). Specifically, we followed a method described in the literature,[44-45] incubating our complexes at a Gd^{3+} concentration of 2.5 mM with 2.5 mM zinc chloride in phosphate buffer ($[PO_4^{3-}]$ = 25 mM) at 37 °C. The concentration of Zn^{2+} used is at least twenty times greater than in plasma; this high concentration makes any difference in transmetallation apparent more rapidly. Upon transmetallation of Gd^{3+} with Zn^{2+}, free Gd^{3+} ions are released and an insoluble $Gd(PO_4)$ complex is formed, preventing rechelation of Gd^{3+} to DOTA. As a control, complexes were incubated without zinc chloride.

For all three DTPA-based contrast agents, r_1 decreases over time, indicating transmetallation with Zn^{2+}. However, the transmetallation in the nanogel is much slower than that of Magnevist® and **1**Gd(III), taking three to five times as long to decrease to 80% of initial r_1, respectively. This indicates that our nanogel PAA/**1**Gd(III) has a slower rate of transmetallation than the other two chelates. After 66 h, the nanogel's r_1 decreased by 23%, compared to ~40% and ~80% decreases for Magnevist® and **1**Gd(III), respectively, suggesting that PAA/**1**Gd(III) transmetallates to a lesser extent. This stability likely results from greater structural rigidity[35] and reduced Zn^{2+} accessibility to chelating sites. In a control experiment without Zn^{2+}, r_1 did not change appreciably for any of the three contrast agents (see Fig. S3). These results suggest that our nanogel, compared to Magnevist® or **1**Gd(III), is more inert against dechelation and is potentially a safer MRI contrast agent.

DOTA-based crosslinkers **2** and **3** and their corresponding nanogels all appear highly stable, with **2**Gd(III) and **3**Gd(III) losing less than 5% of Gd^{3+} over three days. The nanogels' relaxation rate did not decrease at all and instead increased slightly, likely because of evaporation of buffer during the three days of incubation. These results confirm that the incorporation of the crosslinkers into nanogels leads to enhanced stability, which is maximal in the case of the DOTA-based nanogels.

We also examined the contrast provided by all our Gd(III) complexes at 7 T of **1**Gd(III), **2**Gd(III), **3**Gd(III) and their corresponding nanogels PAA/**1**Gd(III), PAA/**2**Gd(III), PAA/**3**Gd(III) by phantom imaging, with Magnevist® and Dotarem® as controls (see Figure S4). At identical gadolinium concentrations, better contrast was obtained with the nanogels compared to either chelated crosslinkers alone or the clinical contrast agents. Therefore, by using such systems, smaller doses of gadolinium would provide similar contrast to that obtained with clinically used contrast agents.

Conclusions

In this article, we have shown that incorporation of gadolinium chelate crosslinkers into nanogels leads to a significant (3 to 4-fold) increase in relaxivity. The relaxivities of the complexed DTPA crosslinker 1Gd(III) and DOTA crosslinkers 2Gd(III) and 3Gd(III) are 4.8 $mM^{-1}s^{-1}$, 4.3 $mM^{-1}s^{-1}$, and 5.0 $mM^{-1}s^{-1}$, respectively, at 60 MHz and 37 °C. When formulated into nanogels, these values rise to 9.7 $mM^{-1}s^{-1}$, 17.6 $mM^{-1}s^{-1}$, and 14.8 $mM^{-1}s^{-1}$, respectively. Importantly, DTPA-based nanogels are thermodynamically and kinetically more inert against transmetallation than Magnevist®, suggesting that crosslinker chelates may represent an important approach towards stable metal-chelating biomedical agents. Moreover, we have reported here the first example of nanogels incorporating a DOTA-based contrast agent as a crosslinker itself. This strategy yields a high relaxivity agent with better contrast than commercial agents and maximal stability toward transmetallation. We are now working on the incorporation of our crosslinkers into nanogels with a biodegradable polymer backbone to allow breakdown into biocompatible small molecules to facilitate clearance. We also plan to use different metals in these chelating crosslinkers to yield nanogels for theranostics combining different imaging modalities such as MRI (Gd^{3+}) and PET (^{64}Cu) with radiotherapy (^{177}Lu).

Supplementary Material

Refer to Web version on PubMed Central for supplementary material.

Acknowledgments

We thank Prof. R. Muller for his help with NMRD measurements. The authors also thank V. A. Nguyen Huu for his help with cell culture and Dr. M. L. Viger for his help with TEM imaging. MC thanks Dr. J. Sankaranarayanan. NMR data was acquired at the UCSD Skaggs School of Pharmacy and Pharmaceutical Sciences NMR Facility. The authors gratefully acknowledge the assistance of staff at the Center for Functional MRI in phantom imaging. LVE and SL thank the Fonds de la Recherche Scientifique (F.N.R.S.) and the ARC, PAI and ENCITE programs for their financial help. This research was made possible by the NIH New Innovator Award (DP 2OD006499), NSF grant 1006081 and KACST (through the KACST-UCSD Center of Excellence in Nanomedicine).

Abbreviations

DCM	dichloromethane
DCC	*N*,*N*′-Dicyclohexylcarbodiimide
DLS	Dynamic Light Scattering
DMAP	4-Dimethylaminopyridine
DMF	dimethylformamide
GBCA	gadolinium-based contrast agents
HR ES-MS	high resolution electrospray mass spectrometry
LC-MS	Liquid Chromatography-Mass Spectrometry
MeOH	Methanol
NMR	nuclear magnetic resonance
ES-MS	electrospray mass spectrometry
NMRD	Nuclear Magnetic Relaxation Dispersion
PAA	polyacrylamide
PTA	Phosphotungstic Acid
TEA	triethylamine
TEM	Transmission Electronic Microscopy
TLC	thin layer chromatography

References

1. Lemieux P, Vinogradov SV, Gebhart CL, Guerin N, Paradis G, Nguyen HK, Ochietti B, Suzdaltseva YG, Bartakova EV, Bronich TK, St-Pierre Y, Alakhov VY, Kabanov AV. J Drug Target. 2000; 8:91–105. [PubMed: 10852341]
2. Kabanov AV, Vinogradov SV. Angew Chem Int Edit. 2009; 48:5418–5429.
3. Bronich TK, Vinogradov SV, Kabanov AV. Nano Lett. 2001; 1:535–540.
4. Missirlis D, Kawamura R, Tirelli N, Hubbell JA. Eur J Pharm Sci. 2006; 29:120–129. [PubMed: 16904301]
5. Kwon YJ, Standley SM, Goh SL, Frechet JMJ. J Control Release. 2005; 105:199–212. [PubMed: 15935507]
6. Standley SM, Mende I, Goh SL, Kwon YJ, Beaudette TT, Engleman EG, Frechet JMJ. Bioconjugate Chem. 2007; 18:77–83.
7. Caravan P, Ellison JJ, McMurry TJ, Lauffer RB. Chem Rev. 1999; 99:2293–2352. [PubMed: 11749483]
8. Mulder WJM, Strijkers GJ, Griffioen AW, van Bloois L, Molema G, Storm G, Koning GA, Nicolay K. Bioconjugate Chem. 2004; 15:799–806.

9. Josephson L, Tung CH, Moore A, Weissleder R. Bioconjugate Chem. 1999; 10:186–191.
10. Mazooz G, Mehlman T, Lai TS, Greenberg CS, Dewhirst MW, Neeman M. Cancer Res. 2005; 65:1369–1375. [PubMed: 15735023]
11. Courant T, Roullin VG, Cadiou C, Callewaert M, Andry MC, Portefaix C, Hoeffel C, de Goltstein MC, Port M, Laurent S, Vander Elst L, Muller R, Molinari M, Chuburu F. Angew Chem Int Edit. 2012; 51:9119–9122.
12. Soleimani A, Martinez F, Economopoulos V, Foster PJ, Scholl TJ, Gillies ER. J Mater Chem B. 2013; 1:1027–1034.
13. Jaszberenyi Z, Moriggi L, Schmidt P, Weidensteiner C, Kneuer R, Merbach AE, Helm L, Toth E. J Biol Inorg Chem. 2007; 12:406–420. [PubMed: 17216229]
14. Nicolle GM, Toth E, Schmitt-Willich H, Raduchel B, Merbach AE. Chem-Eur J. 2002; 8:1040–1048. [PubMed: 11891890]
15. Rudovsky J, Hermann P, Botta M, Aime S, Lukes I. Chem Commun. 2005:2390–2392.
16. Floyd WC, Klemm PJ, Smiles DE, Kohlgruber AC, Pierre VC, Mynar JL, Frechet JMJ, Raymond KN. J Am Chem Soc. 2011; 133:2390–2393. [PubMed: 21294571]
17. Schopf E, Sankaranarayanan J, Chan M, Mattrey R, Almutairi A. Mol Pharmaceut. 2012; 9:1911–1918.
18. Lebduskova P, Kotek J, Hermann P, Vander Elst L, Muller RN, Lukes I, Peters JA. Bioconjugate Chem. 2004; 15:881–889.
19. Corsi DM, Vander Elst L, Muller RN, van Bekkum H, Peters JA. Chem-Eur J. 2001; 7:1383–1389. [PubMed: 11330890]
20. Kielar F, Tei L, Terreno E, Botta M. J Am Chem Soc. 2010; 132:7836–+. [PubMed: 20481537]
21. Zhang GD, Zhang R, Wen XX, Li L, Li C. Biomacromolecules. 2008; 9:36–42. [PubMed: 18047289]
22. Verwilst P, Eliseeva SV, Vander Elst L, Burtea C, Laurent S, Petoud S, Muller RN, Parac-Vogt TN, De Borggraeve WM. Inorg Chem. 2012; 51:6405–6411. [PubMed: 22583122]
23. Gebhart CL, Sriadibhatla S, Vinogradov S, Lemieux P, Alakhov V, Kabanov AV. Bioconjugate Chem. 2002; 13:937–944.
24. Lux F, Mignot A, Mowat P, Louis C, Dufort S, Bernhard C, Denat F, Boschetti F, Brunet C, Antoine R, Dugourd P, Laurent S, Vander Elst L, Muller R, Sancey L, Josserand V, Coll JL, Stupar V, Barbier E, Remy C, Broisat A, Ghezzi C, Le Duc G, Roux S, Perriat P, Tillement O. Angew Chem Int Edit. 2011; 50:12299–12303.
25. Morlieras J, Chezal JM, Miot-Noirault E, Roux A, Heinrich-Balard L, Cohen R, Tarrit S, Truillet C, Mignot A, Hachani R, Kryza D, Antoine R, Dugourd P, Perriat P, Janier M, Sancey L, Lux F, Tillement O. Nanoscale. 2013; 5:1603–1615. [PubMed: 23334308]
26. Anderson EA, Isaacman S, Peabody DS, Wang EY, Canary JW, Kirshenbaum K. Nano Lett. 2006; 6:1160–1164. [PubMed: 16771573]
27. Prasuhn DE, Yeh RM, Obenaus A, Manchester M, Finn MG. Chem Commun. 2007:1269–1271.
28. Nicolle GM, Toth E, Eisenwiener KP, Macke HR, Merbach AE. J Biol Inorg Chem. 2002; 7:757–769. [PubMed: 12203012]
29. Allen M, Bulte JWM, Liepold L, Basu G, Zywicke HA, Frank JA, Young M, Douglas T. Magn Reson Med. 2005; 54:807–812. [PubMed: 16155869]
30. Garimella PD, Datta A, Romanini DW, Raymond KN, Francis MB. J Am Chem Soc. 2011; 133:14704–14709. [PubMed: 21800868]
31. Caravan P, Cloutier NJ, Greenfield MT, McDermid SA, Dunham SU, Bulte JWM, Amedio JC, Looby RJ, Supkowski RM, Horrocks WD, McMurry TJ, Lauffer RB. J Am Chem Soc. 2002; 124:3152–3162. [PubMed: 11902904]
32. Caravan P, Parigi G, Chasse JM, Cloutier NJ, Ellison JJ, Lauffer RB, Luchinat C, McDermid SA, Spiller M, McMurry TJ. Inorg Chem. 2007; 46:6632–6639. [PubMed: 17625839]
33. Henoumont C, Henrotte V, Laurent S, Vander Elst L, Muller RN. J Inorg Biochem. 2008; 102:721–730. [PubMed: 18096235]
34. Guo ZJ, Sadler PJ. Angew Chem Int Edit. 1999; 38:1513–1531.

35. Port M, Idee JM, Medina C, Robic C, Sabatou M, Corot C. Biometals. 2008; 21:469–490. [PubMed: 18344005]
36. Manus LM, Strauch RC, Hung AH, Eckermann AL, Meade TJ. Anal Chem. 2012; 84:6278–6287. [PubMed: 22624599]
37. Urbanczyk-Pearson LM, Femia FJ, Smith J, Parigi G, Duimstra JA, Eckermann AL, Luchinat C, Meade TJ. Inorg Chem. 2008; 47:56–68. [PubMed: 18072754]
38. Bonnet CS, Buron F, Caille F, Shade CM, Drahos B, Pellegatti L, Zhang J, Villette S, Helm L, Pichon C, Suzenet F, Petoud S, Toth E. Chem-Eur J. 2012; 18:1419–1431. [PubMed: 22213187]
39. Caille F, Bonnet CS, Buron F, Villette S, Helm L, Petoud S, Suzenet F, Toth E. Inorg Chem. 2012; 51:2522–2532. [PubMed: 22233349]
40. Ochietti B, Lemieux P, Kabanov AV, Vinogradov S, St-Pierre Y, Alakhov V. Gene Ther. 2002; 9:939–945. [PubMed: 12085242]
41. Powell DH, NiDhubhghaill OM, Pubanz D, Helm L, Lebedev YS, Schlaepfer W, Merbach AE. J Am Chem Soc. 1996; 118:9333–9346.
42. Toth E, Helm L, Merbach AE. Top Curr Chem. 2002; 221:61–101.
43. Aime S, Caravan P. J Magn Reson Imaging. 2009; 30:1259–1267. [PubMed: 19938038]
44. Robic C, Catoen S, Goltstein DM, Idée J, Port M. Biometals. 2011; 24:759–768. [PubMed: 21390525]
45. Laurent S, Vander Elst L, Henoumont C, Muller RN. Contrast Media Mol I. 2010; 5:305–308.

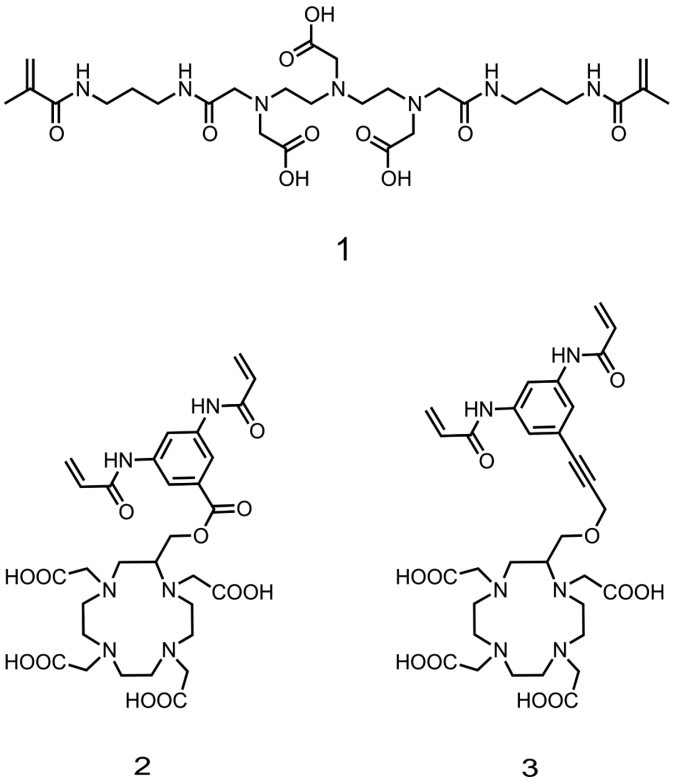

Figure 1.
Chemical structures of the target DTPA and DOTA-based crosslinkers **1**, **2** and **3**.

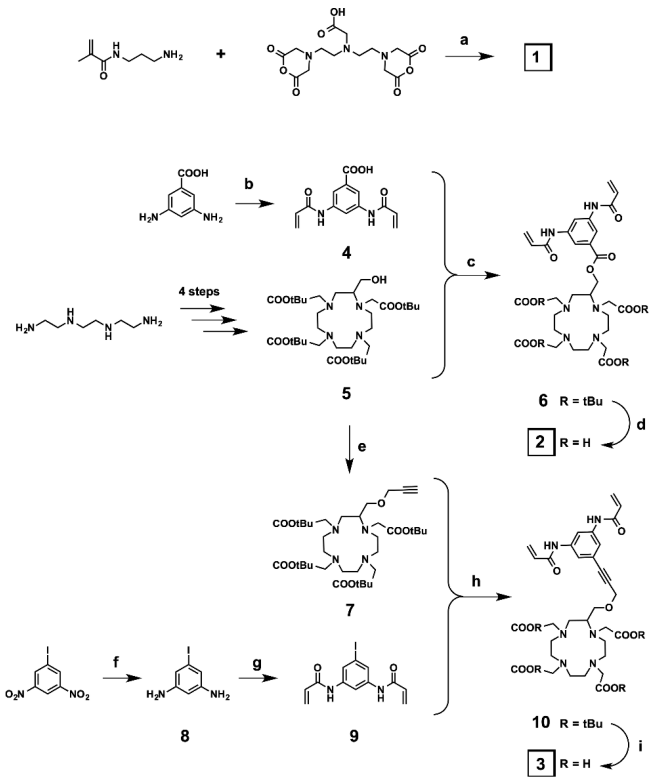

Scheme 1.

Synthesis of crosslinkers 1, 2 and 3. a) Et_3N, r.t., 24 h, 61%; b) acryloyl chloride, K_2CO_3, EtOAc/H2O, 0 °C to r.t., 30 min, 73%; c) DCC, DMAP, DCM, 0 °C to r.t., 48 h, 59%; d) TFA/DCM 1:1, r.t., 16 h, 100%; e) propargyl bromide, tetrabutylammonium iodide, CsOH, DCM, 0 °C to r.t., 1 h, 75%; f) $SnCl_2.(H_2O)_2$, 70 °C, 30 min, 100%; g) acryloyl chloride, EtOAc/H2O, 0 °C to r.t., 10 min, 100%; h) $Pd(PPh_3)_2Cl_2$, CuI, Et_3N, THF, 50 °C, 48 h, 59%; i) TFA, r.t., 4 h, 45%.

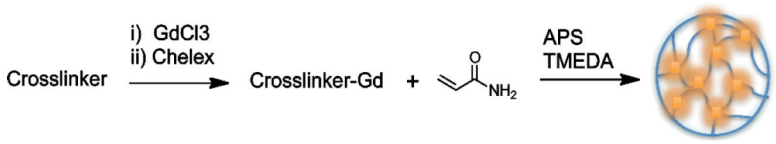

Figure 2.
Preparation of nanogels through inverse emulsion process.

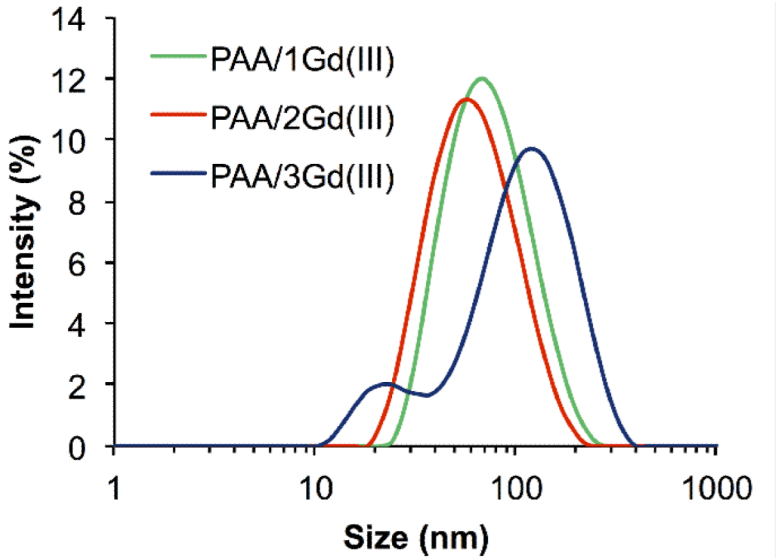

Figure 3.
Size distribution of PAA/**1**Gd(III), PAA/**2**Gd(III) and PAA/**3**Gd(III) nanogels as measured by dynamic light scattering.

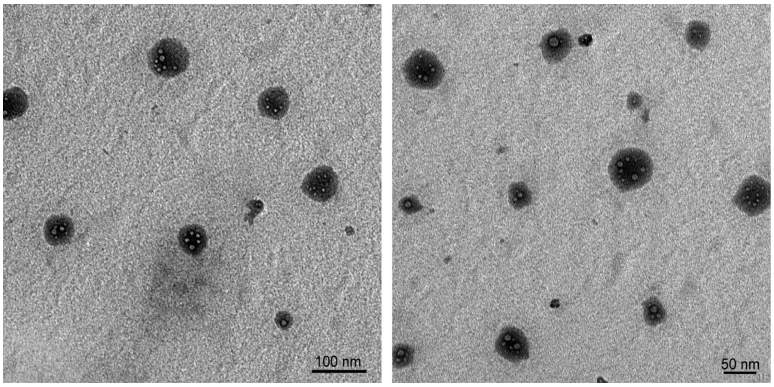

Figure 4.
TEM microphotographs of polyacrylamide nanogels with Gd^{3+}-chelating crosslinkers PAA/**2**Gd(III)..

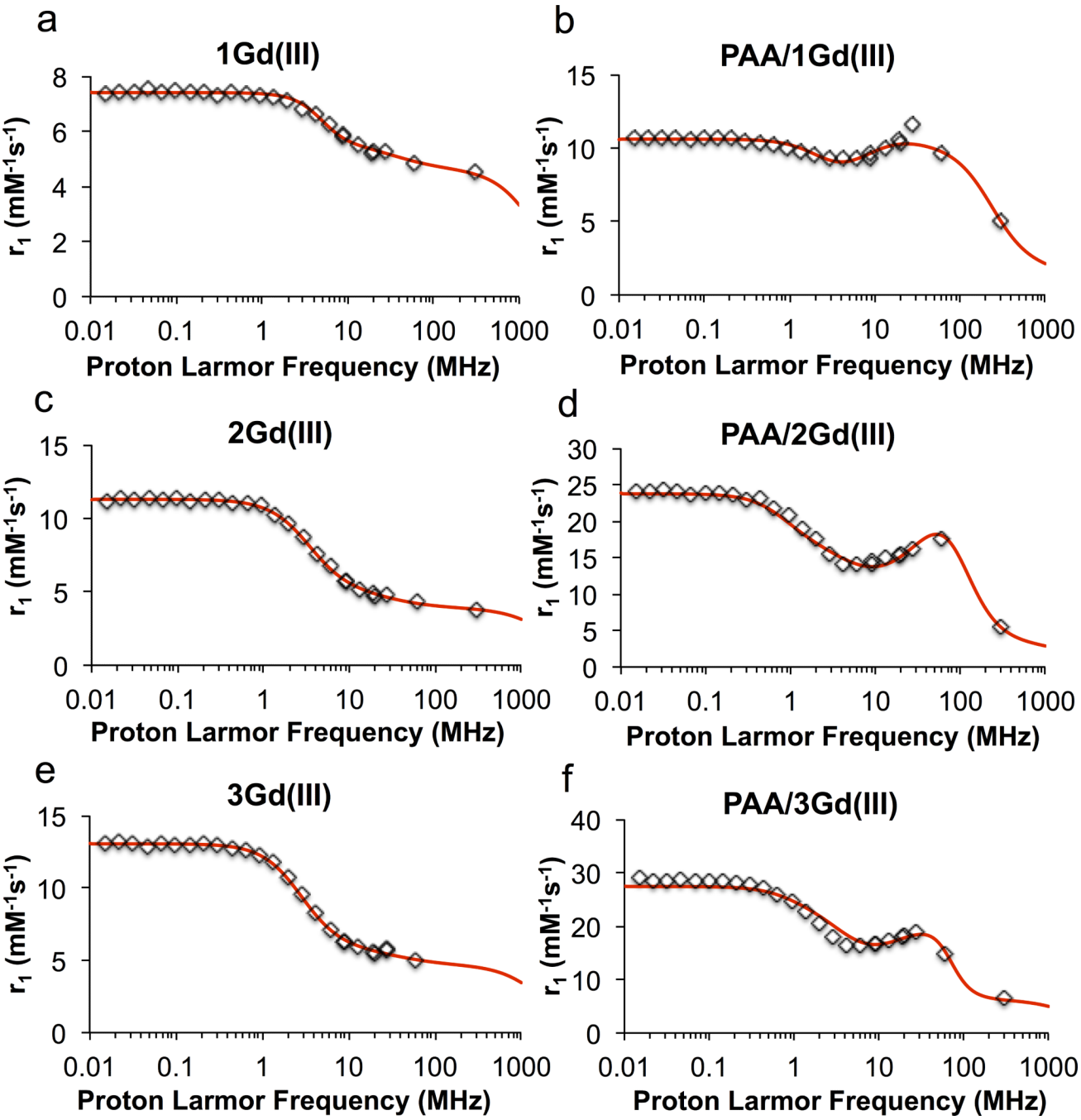

Figure 5.

NMRD profiles of the chelated crosslinkers a) **1**Gd(III), c) **2**Gd(III) e) **3**Gd(III) and their corresponding PAA nanogels b) PAA/**1**Gd(III), d) PAA/**2**Gd(III) and f) PAA/**3**Gd(III). The relaxivity measurements were performed at 37 °C. Data points shown in rhombus and fitted curve in solid line.

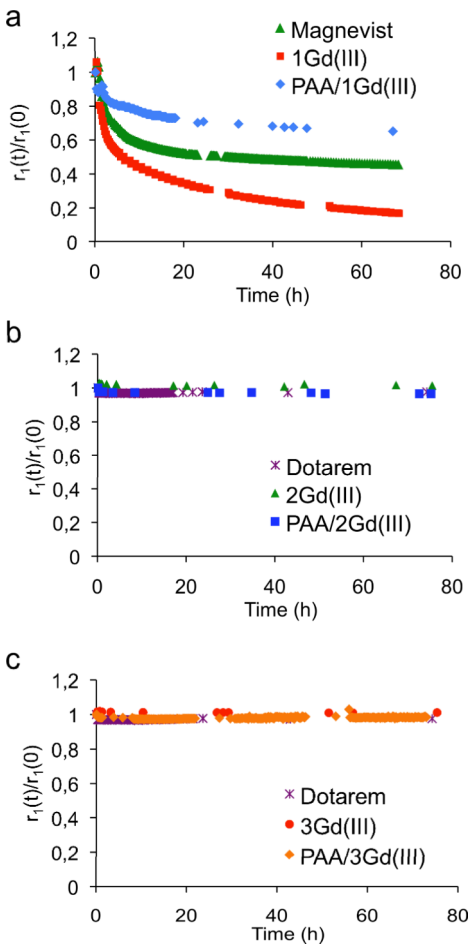

Figure 6.

Stability of the Gd^{3+} complexes of a) DTPA-based crosslinker **1** and its corresponding PAA nanogel, b) DOTA-based crosslinker **2** and its corresponding PAA nanogel, and c) DOTA-based crosslinker **3** and its corresponding PAA nanogel. Experiments were carried out in phosphate buffer with 2.5 mM $ZnCl_2$ at 37 °C and pH 7.4. Control experiments were carried out in the absence of $ZnCl_2$ (see Figure S3).